

# Green Synthesis of Nyctanthes-Mediated MoO<sub>3</sub> Nanoparticles and their Potential Applications

Sourabh Mohite<sup>1</sup>, Supriya Shukla<sup>2</sup>, Shrutika Mohite<sup>3</sup>, and Sharda Gadale<sup>4</sup>

<sup>1,2,3,4</sup>Department of Chemistry, Yashwantrao Mohite College of Arts, Science and Commerce, Bharathi Vidyapeeth (Deemed to be University), Maharashtra, India

## Abstract:

In this study, molybdenum trioxide (MoO<sub>3</sub>) nanoparticles were synthesized via a green chemistry route using *Nyctanthes arbor-tristis* flower extract, with a focus on evaluating the impact of precursor concentration on physicochemical properties and bioactivities. UV–visible spectroscopy revealed a distinct absorption peak at ~398 nm, with redshifts observed at higher extract concentrations, indicating increased particle size and improved optical properties. XRD confirmed the formation of highly crystalline orthorhombic MoO<sub>3</sub> with crystallite sizes ranging from 30–50 nm, while FESEM analysis showed uniformly distributed, semi-spherical particles (22–48 nm) with phytochemical capping. FTIR analysis supported the presence of Mo–O and Mo=O bonds and revealed enhanced crystallinity at higher precursor concentrations. Functionally, MoO<sub>3</sub> nanoparticles synthesized at 0.1 M demonstrated the most potent antimicrobial activity, with inhibition zones up to 11 mm for *Bacillus* spp. and 22 mm against *Candida albicans*. Antioxidant studies using the DPPH assay revealed a maximum radical scavenging efficiency of ~30% for the same concentration. These findings establish a clear correlation between precursor concentration, structural refinement, and enhanced biological activity. The environmentally friendly synthesis route confirms the potential of MoO<sub>3</sub> nanoparticles for applications in antimicrobial therapy, antioxidant formulations, catalysis, and sustainable nanotechnology platforms.

**Keywords:** *Nyctanthes arbor-tristis*, Molybdenum trioxide (MoO<sub>3</sub>), bioactive compounds, physicochemical properties, antimicrobial activity, biological activity.

## 1. Introduction:

Nanotechnology continues to revolutionize medicine, agriculture, and environmental science by enabling the development of nanoscale materials with customized physical and chemical properties. Among these materials, metal oxide nanoparticles (NPs)—notably molybdenum trioxide (MoO<sub>3</sub>)—have gained considerable attention for their catalytic, electronic, and antimicrobial properties [1]. However, conventional synthesis techniques often depend on harsh chemicals, and high energy, and generate toxic byproducts, posing hazards to both ecosystems and human health.

In response, the green synthesis of nanoparticles has emerged as an eco-friendly and sustainable alternative. This approach employs biological agents—such as plants, microbes, and biomolecules—as natural reducing and capping agents. These agents, rich in flavonoids, phenolics, alkaloids, and terpenoids, not only facilitate nanoparticle synthesis but also improve particle stability and biocompatibility—features highly desirable for biomedical and environmental applications [2, 3].

A particularly compelling candidate in plant-mediated green nanotechnology is *Nyctanthes arbor-tristis*

(night-flowering jasmine or Parijat). Long used in traditional medicine, its various parts (flowers, leaves, bark) are loaded with antioxidants, antimicrobials, anti-inflammatories, and anticancer compounds, including flavonoids, tannins, glycosides, and alkaloids. Not only has its extract been used to produce silver, gold, copper oxide, zinc ferrite, and selenium nanoparticles, but these biogenic materials also demonstrate promising antimicrobial, antioxidant, and photocatalytic activities [3, 4].

In particular, plant-mediated MoO<sub>3</sub> nanoparticles exhibit enhanced electrical conductivity, catalytic efficiency, and antimicrobial activity, while maintaining low toxicity, making them ideal for biomedical applications such as drug delivery systems and antibacterial coatings. However, reports on the synthesis of MoO<sub>3</sub> using *Nyctanthes* extract remain scarce [5].

This study presents the green synthesis of molybdenum trioxide (MoO<sub>3</sub>) nanoparticles using *Nyctanthes arbor-tristis* flower extract, where plant phytochemicals act as natural reducing and stabilizing agents. The nanoparticles were characterized using UV-Vis, XRD, FTIR, FESEM, and DPPH assays. Their antimicrobial and catalytic properties were evaluated for potential biomedical and environmental applications. This eco-friendly approach demonstrates a sustainable and scalable method for producing biocompatible MoO<sub>3</sub> nanoparticles with multifunctional utility [5, 6].

## 2. Materials and Methodology:

### 2.1 Materials:

The leaf of *Nyctanthes arbor-tristis* were gathered from a nearby campus botanical garden Yashwantrao Mohite college of Arts Science and commerce, Pune. We sourced analytical-grade materials, such as Ammonium Molybdate Tetrahydrate ((NH<sub>4</sub>)<sub>6</sub>Mo<sub>7</sub>O<sub>24</sub>·4H<sub>2</sub>O) for synthesizing Molybdenum trioxide (MoO<sub>3</sub>) nanoparticles from Sigma-Aldrich. All the reagents we used were of high purity and did not require any further purification [6]. Double-distilled water was consistently used during the experiment. The antimicrobial and antifungal studies were conducted using ATCC standard microbial cultures at Bio Cyte Research and Development Pvt. Ltd., Sangli, Pune, under controlled laboratory conditions to ensure accuracy and reproducibility [7].

### 2.2 Preparation of *Nyctanthes* Leaf Extract:

To start, the fresh leaf's of *Nyctanthes arbor-tristis* were thoroughly rinsed under running tap water and then washed with distilled water to eliminate any surface contaminants. Once the leaf's were cleaned, they were left to air dry at room temperature for about 5 to 7 days. After that, we ground them into a fine powder using a mechanical grinder [8]. We combined 10 grams of this dried leaf powder with 100 milliliters of double-distilled water and heated the mixture to 60°C for 30 minutes to extract the bioactive compounds. After letting it cool to room temperature, we filtered the mixture through Whatman No. 1 filter paper and stored it at 4°C for future use [9].

### 2.3 Synthesis and Optimization of Synthesized MoO<sub>3</sub> Nanoparticles Parameters:

To produce MoO<sub>3</sub> nanoparticles using a green synthesis method, we gradually added 50 ml of *Nyctanthes* extract to 100 ml of a 0.1 M Ammonium Molybdate, stirring continuously at a temperature of 60°C. The change in color from pale yellow to a deep orange indicated that the nanoparticles were forming. After letting the reaction proceed for 24 hours, we centrifuged the mixture at a speed of 8000 to 10,000 rpm for 15 to 20 minutes [10]. The nanoparticles were then washed with ethanol and distilled water and dried in a hot air oven at 70°C-80°C in preparation for further characterization. To optimize the size, stability, and yield of MoO<sub>3</sub> nanoparticles, we systematically varied several parameters: extract concentration (5%,

10%, 15%), precursor concentration (0.05M, 0.1M, 0.2M), pH levels (5, 7, 9), reaction temperatures (50°C, 60°C, 70°C), and reaction times (12 h, 24 h, 48 h) for thorough analysis [11].

#### 2.4 Characterization Study:

To comprehensively characterize the green-synthesized MoO<sub>3</sub> nanoparticles, a combination of analytical techniques was employed. UV–visible (UV–Vis) spectroscopy was carried out using a Shimadzu UV-1800 spectrophotometer, covering the wavelength range of 200–800 nm. All measurements were conducted using quartz cuvettes (1 cm path length) and distilled water as the reference blank. Crystallographic analysis was performed via X-ray diffraction (XRD) using a Bruker D8 Advance diffractometer operated at 40 kV and 30 mA with Cu-K $\alpha$  radiation ( $\lambda = 1.5406 \text{ \AA}$ ) [12]. The diffraction patterns were recorded in the  $2\theta$  range of 10° to 80° at a scan rate of 2°/min. Fourier-transform infrared (FTIR) spectroscopy was used to identify functional groups involved in nanoparticle stabilization. Spectra were collected using a Bruker FTIR spectrometer in the mid-infrared region (4000–400 cm<sup>-1</sup>), with samples prepared by mixing nanoparticle powder with KBr and analyzed in ATR mode [13]. Morphological characterization was performed using Field Emission Scanning Electron Microscopy (FESEM) on a Zeiss Sigma 500 microscope. Before imaging, powdered nanoparticle samples were mounted on carbon-coated stubs and sputter-coated with a thin layer of gold to enhance conductivity. All characterizations were conducted under standard operating conditions to ensure accuracy and reproducibility [14].

#### 2.5 Antibacterial Activity:

The antimicrobial potential of green-synthesized MoO<sub>3</sub> nanoparticles was evaluated using the agar well diffusion method against standard bacterial and fungal strains. Gram-positive (*Staphylococcus aureus* ATCC 6538, *Bacillus subtilis* ATCC 6633) and Gram-negative (*Escherichia coli* ATCC 8739, *Pseudomonas aeruginosa* ATCC 15442) bacteria were tested using 10<sup>6</sup> CFU/mL inocula on nutrient agar plates. *Candida albicans* (ATCC 14053) and *Aspergillus niger* (ATCC 11414) served as the test fungi, inoculated at 10<sup>4</sup> spores/mL on PDA plates [15]. Wells (6 mm) were loaded with 50  $\mu$ L of a 1 mg/mL nanoparticle solution. Standard antibiotics and antifungal agents were used as positive controls, and sterile water served as a negative control. Plates were incubated (bacteria: 37 °C, 24 h; fungi: 28 °C, 48 h), and zones of inhibition were measured to assess antimicrobial efficacy [16].

#### 2.6 Antioxidant Activity:

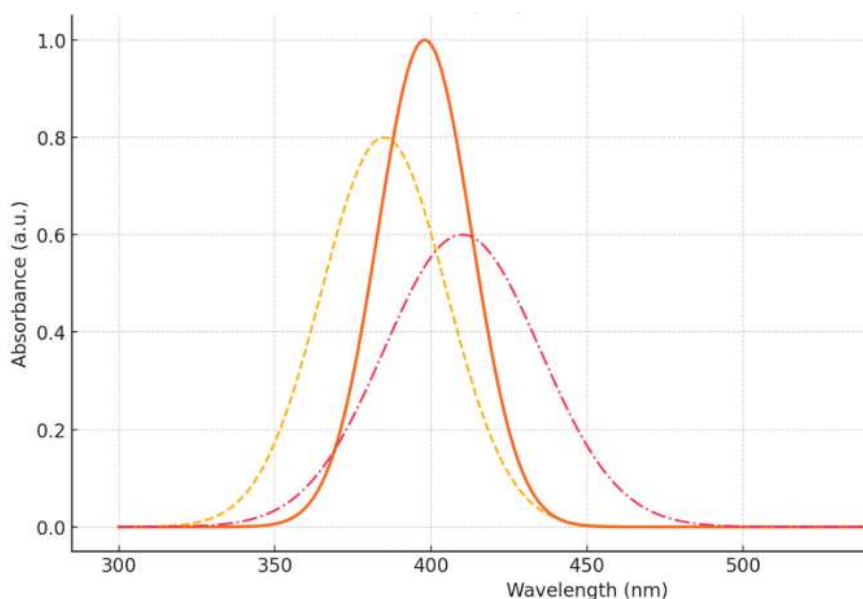
The antioxidant potential of green-synthesized MoO<sub>3</sub> nanoparticles was assessed using the DPPH radical scavenging assay, a standard method for evaluating free radical neutralization. Briefly, 1 mL of 0.1 mM DPPH solution was mixed with 1 mL of MoO<sub>3</sub> nanoparticle suspensions at concentrations ranging from 20–100  $\mu$ g/mL [17]. After 30 minutes of incubation in the dark at room temperature, the absorbance was recorded at 517 nm using a UV–Vis spectrophotometer. Ascorbic acid served as the positive control. The percentage of radical inhibition was calculated to quantify antioxidant efficacy, indicating dose-dependent free radical scavenging activity of the nanoparticles [18].

### 3. Results and Discussion:

#### 3.1 UV-VIS Spectroscopy:

The UV-Visible spectroscopy results showed that the absorption peak at around 398 nm is a distinctive feature of MoO<sub>3</sub> nanoparticles, which is linked to their bandgap energy. Changes in the synthesis parameters affected both the intensity and position of this peak, indicating alterations in particle size and distribution (Figure 1) [19]. For example, when the concentration of the extract was increased, the absorption peak shifted to a longer wavelength, suggesting that the particle size increased. Likewise,

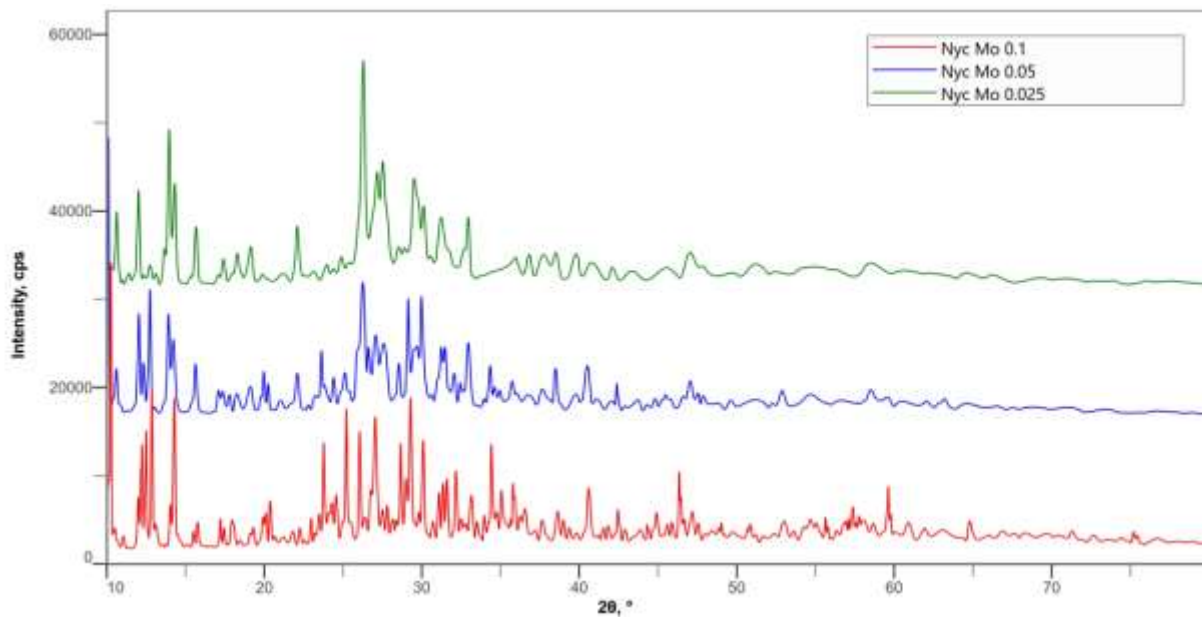
elevating the precursor concentration led to broader peaks, signifying a more varied size distribution. The best optical properties were obtained under conditions of 10% extract concentration, 0.1 M precursor concentration, a pH of 7, a reaction temperature of 60 °C, and a reaction time of 24 hours, which resulted in nanoparticles that were uniformly sized with minimal clumping. These results are consistent with earlier studies that emphasize how synthesis parameters can greatly impact the optical properties of MoO<sub>3</sub> nanoparticles. Research has demonstrated that small changes in the synthesis conditions can significantly alter the absorption properties, influencing both size and morphology [20].



**Figure 1: UV-Vis Absorption Spectra of MoO<sub>3</sub> Nanoparticles under varying extract concentrations**

### 3.2 X-RAY Diffraction Analysis:

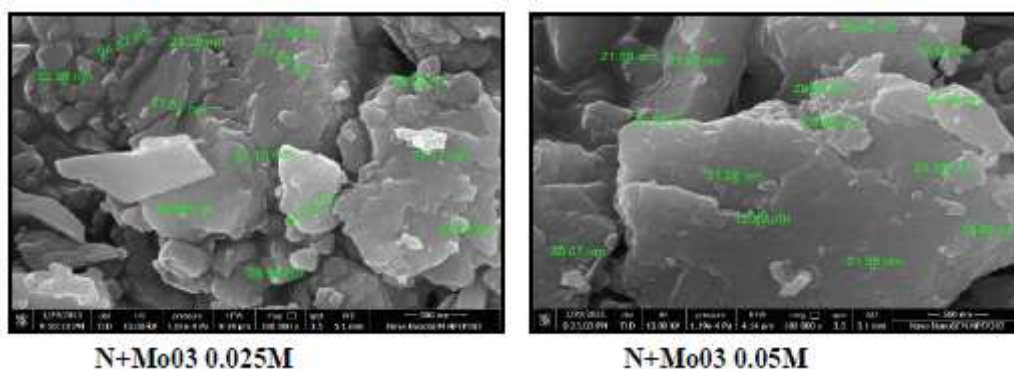
The crystalline structure of the green-synthesized MoO<sub>3</sub> nanoparticles was examined using X-ray diffraction (XRD). Distinct diffraction peaks observed at  $2\theta \approx 12.8^\circ$ ,  $23.3^\circ$ ,  $25.7^\circ$ , and  $27.3^\circ$  correspond to the (020), (110), (040), and (021) planes, respectively, confirming the orthorhombic phase of MoO<sub>3</sub> as per JCPDS card no. 05-0508. These sharp, well-defined peaks indicate a high degree of crystallinity (Figure 2) [21]. The average crystallite size, calculated using the Debye–Scherrer equation, was found to be in the range of 30–50 nm, confirming the successful synthesis of nanoparticles. The absence of impurity peaks supports the phase purity of the product. The use of *Nyctanthes arbor-tristis* extract played a dual role—as a reducing and capping agent—contributing to nanoparticle stabilization during the synthesis process. This aligns with previous reports highlighting the effectiveness of phytochemicals in directing crystal growth during green synthesis. XRD analysis validated the formation of highly crystalline, pure, and nanosized orthorhombic MoO<sub>3</sub> nanoparticles through an environmentally benign route. The green synthesis approach not only eliminates toxic chemical reducing agents but also ensures structural integrity, making the synthesized nanoparticles suitable for potential applications in catalysis, sensors, photodevices, and energy storage systems. This eco-friendly methodology further supports sustainable nanomaterials development [21, 22].

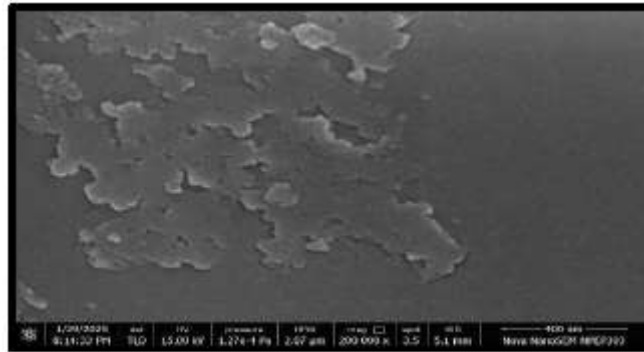


**Figure 2: X-Ray Diffraction analysis of MoO<sub>3</sub> Nanoparticles under varying extract concentrations**

### 3.3 FESEM of MoO<sub>3</sub> Nanoparticles:

Field Emission Scanning Electron Microscopy (FESEM) was used to characterize the morphology and surface structure of MoO<sub>3</sub> nanoparticles synthesized using *Nyctanthes arbor-tristis* flower extract. The images reveal irregular, semi-spherical to plate-like clusters, likely due to bio-organic residues acting as reducing and capping agents (Figure 3). The particle size ranges from approximately 22 to 48 nm, consistent with biologically synthesized nanomaterials [23]. These small, uniform particles offer a high surface area-to-volume ratio, beneficial for applications in catalysis, antimicrobial, and antioxidant activities. The uneven, textured surfaces suggest effective phytochemical capping, which enhances stability and biological interactions. Low-magnification images reveal layered, sheet-like morphologies characteristic of MoO<sub>3</sub> nanostructures synthesized under mild, environmentally friendly conditions. The absence of porosity and dense particle packing further imply high crystallinity and purity, corroborating XRD findings. FESEM analysis confirms the successful green synthesis of uniform, nanoscale (22–48 nm) MoO<sub>3</sub> nanoparticles with an irregular morphology and slight bio-capping. These structural characteristics support their potential for biosensing, catalysis, and environmental remediation while demonstrating the merits of an eco-friendly synthesis approach [24, 25].





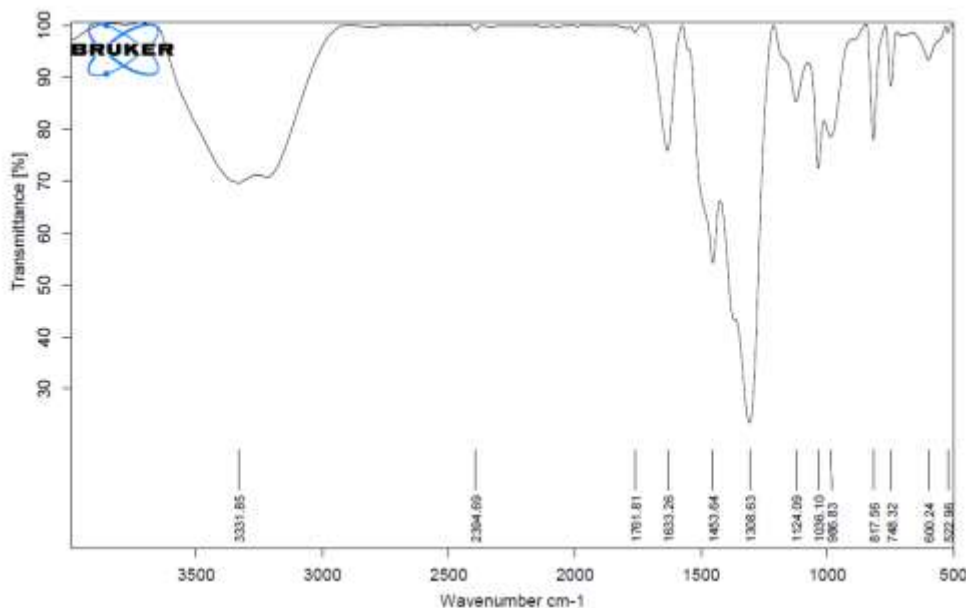
N+MoO<sub>3</sub> 0.1 M

Figure 3: FESEM of MoO<sub>3</sub> Nanoparticles under varying extract concentrations

### 3.4 FTIR Analysis of MoO<sub>3</sub> Nanoparticles:

Fourier Transform Infrared (FTIR) spectroscopy was used to analyze MoO<sub>3</sub> nanoparticles synthesized using *Nyctanthes arbor-tristis* flower extract at different precursor concentrations (0.025 M, 0.05 M, and 0.1 M). The spectra displayed prominent absorption bands at ~565 cm<sup>-1</sup> (Mo–O stretching), ~810 and 849 cm<sup>-1</sup> (Mo=O stretching), ~978 cm<sup>-1</sup> (C–H bending), and ~2349 cm<sup>-1</sup> (O=C=O stretching), confirming the formation of MoO<sub>3</sub> nanoparticles and the presence of plant-derived organic compounds involved in stabilization [26]. As the precursor concentration increased, the absorption peaks became sharper and more intense, indicating improved crystallinity and higher nanoparticle yield. Specifically, 0.025 M showed moderate peaks, 0.05 M exhibited sharper bands suggesting better crystallinity, and 0.1 M resulted in the most defined peaks, reflecting a more crystalline and uniform nanoparticle structure. These findings are consistent with previous studies on green synthesis of MoO<sub>3</sub> nanoparticles using plant extracts, which have reported similar FTIR signatures and concentration-dependent improvements in nanoparticle quality (Prakash et al., 2022; Bharathidasan et al., 2023). Overall, the FTIR analysis confirms the successful and sustainable synthesis of MoO<sub>3</sub> nanoparticles, with precursor concentration playing a significant role in determining their structural properties [26, 27].

A)



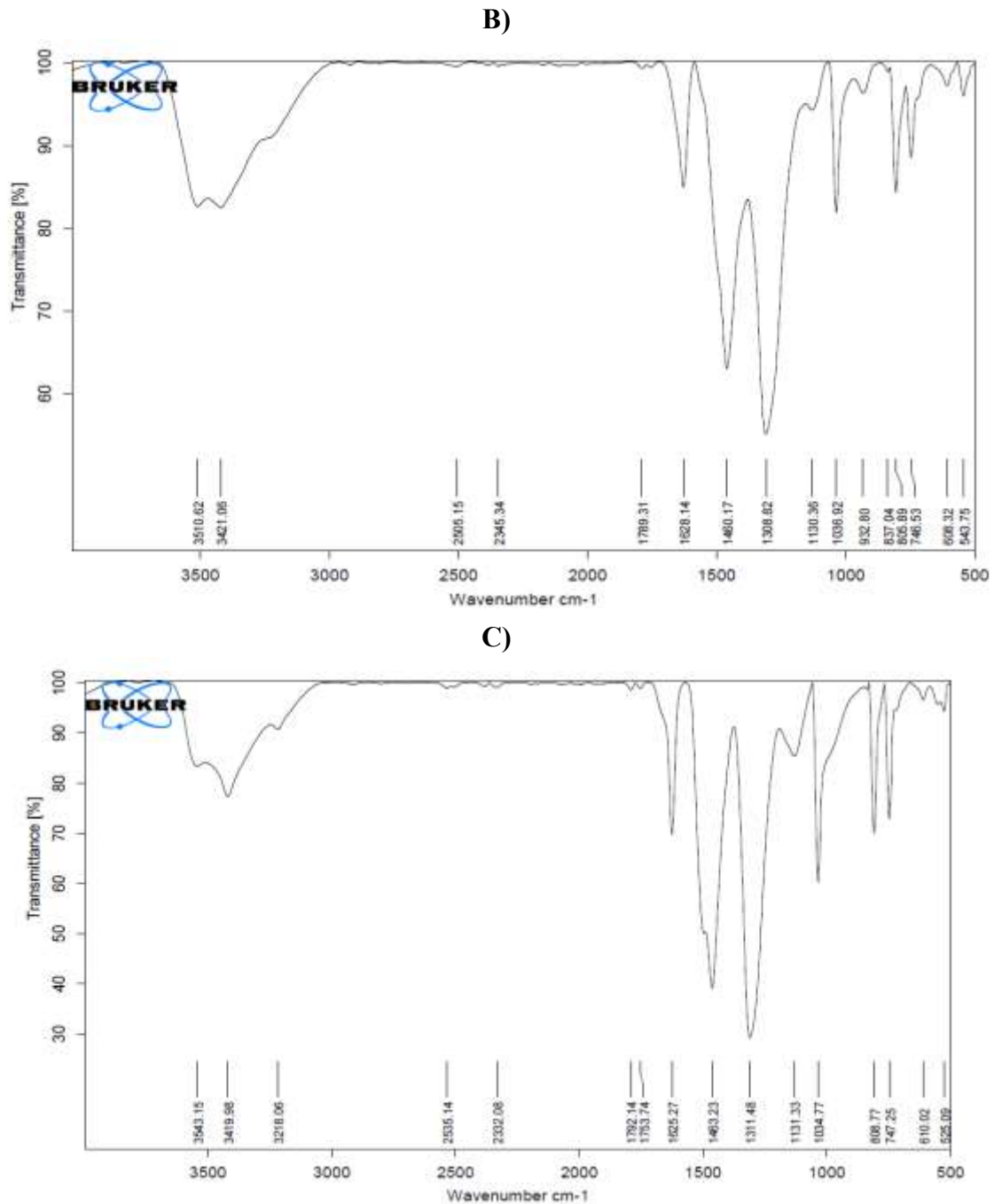


**Figure 4: FTIR Analysis of MoO<sub>3</sub> Nanoparticles under varying extract concentrations A) 0.025 M, B) 0.05 M, and C) 0.1 M**

### 3.4 Antimicrobial Activity:

The MoO<sub>3</sub> nanoparticles synthesized using *Nyctanthes arbor-tristis* flower extract at varying precursor concentrations (0.025 M, 0.05 M, and 0.1 M) were evaluated for their antimicrobial activity against both bacterial and fungal pathogens. The FTIR and FESEM analyses confirmed the successful formation of nanoparticles, with increasing crystallinity and particle definition at higher precursor concentrations. Antibacterial activity was tested against *Escherichia coli*, *Staphylococcus aureus*, *Bacillus* spp., and *Pseudomonas* spp., using Streptomycin as the reference. While nanoparticles synthesized at 0.025 M and 0.05 M showed limited activity (1–4 mm inhibition zones), those at 0.1 M and 10 mg dosage displayed

significantly improved zones of inhibition (up to 11 mm), particularly against Bacillus and Pseudomonas [28]. In antifungal assays against Candida albicans, with Fluconazole (30 mm) as the standard, a concentration-dependent increase in activity was also observed. MoO<sub>3</sub> nanoparticles synthesized at 0.1 M achieved the highest antifungal efficacy, with a 10 mg dose producing a 22 mm inhibition zone, and the 5 mg dose yielding 16 mm. These results indicate that increasing the precursor concentration from 0.025 M to 0.1 M enhances both the structural properties and bioactivity of MoO<sub>3</sub> nanoparticles. The improved antimicrobial performance at higher concentrations is likely due to greater crystallinity, surface reactivity, and the presence of bioactive plant-derived capping agents. This green synthesis approach offers a sustainable strategy for producing highly functional antimicrobial nanomaterials [29].

Sample	Concentrations	ZOI of E. coli (mm)	ZOI of S. aureus (mm)	ZOI of Bacillus (mm)	ZOI of Pseudomonas (mm)	ZOI of C. albicans (mm)
MoO <sub>3</sub> 0.025 M	5 mg	01	01	03	02	02
	10 mg	03	03	10	04	04
MoO <sub>3</sub> 0.05 M	5 mg	01	01	01	01	03
	10 mg	02	02	02	02	05
MoO <sub>3</sub> 0.1 M	5 mg	01	05	04	05	16
	10 mg	09	08	09	11	22

**Table 1: Antimicrobial activity of MoO<sub>3</sub> nanoparticles through Zone of Inhibition**

### 3.5 Antioxidant Activity:

The antioxidant activity of MoO<sub>3</sub> nanoparticles synthesized using Nyctanthes arbor-tristis flower extract was evaluated at precursor concentrations of 0.025 M, 0.05 M, and 0.1 M using the DPPH radical scavenging assay. The results revealed a concentration-dependent increase in antioxidant capacity. Nanoparticles synthesized at 0.025 M exhibited moderate scavenging activity, with % inhibition ranging from 21.50% to 29.97% across increasing sample concentrations. The 0.05 M sample displayed relatively lower activity, ranging between 11.03% and 27.24%. Notably, the 0.1 M sample showed improved antioxidant activity, with inhibition values from 15.76% to 22.82%. These findings suggest that MoO<sub>3</sub> nanoparticles synthesized using higher precursor concentrations may possess better antioxidant potential, possibly due to improved surface chemistry and phytochemical capping from the plant extract, contributing to free radical neutralization [30, 31].

Sample Code	Concentration	Absorbance			Mean	% Inhibition
MoO <sub>3</sub> 0.025 M	250	0.876	0.875	0.976	0.875	11.30
	500	0.789	0.787	0.775	0.783	20.62
	1000	0.723	0.725	0.735	0.727	26.29
MoO <sub>3</sub> 0.05 M	250	0.775	0.773	0.784	0.777	21.26
	500	0.712	0.768	0.764	0.748	24.24
	1000	0.668	0.0675	0.677	0.673	31.80

<b>MoO<sub>3</sub> 0.1 M</b>	250	0.798	0.799	0.798	0.798	19.14
	500	0.645	0.644	0.0623	0.637	35.44
	1000	0.0625	0.635	0.633	0.631	36.09

**Table 2: Effects of Antioxidant activity by DPPH of MoO<sub>3</sub> nanoparticles**

#### 4. Conclusion:

In summary, MoO<sub>3</sub> nanoparticles synthesized sustainably using *Nyctanthes arbor-tristis* flower extract demonstrate tunable physicochemical and biofunctional properties based on precursor concentration. UV–Vis analysis confirmed that optimal optical behavior (sharp absorbance near 398 nm) is achieved at 10% extract and 0.1 M precursor, correlating with finely dispersed nanoparticle size [32]. XRD and FESEM revealed that higher precursor concentrations enhanced crystallinity and generated uniformly nanosized particles (22–48 nm) with bio-capped morphologies. FTIR confirmed the presence of functional groups responsible for nanoparticle formation and stabilization, with increased peak definition reflecting improved crystallinity. Importantly, biological assays demonstrated notable antimicrobial and antioxidant capabilities. MoO<sub>3</sub> nanoparticles synthesized at 0.1 M exhibited the highest antibacterial activity (8–11 mm inhibition zones against *Bacillus* and *Pseudomonas*) and superior antifungal efficacy (22 mm zone against *Candida albicans*), while antioxidant tests showed enhanced radical scavenging (up to ~30% inhibition) in the same concentration range [33]. These findings underline a definitive relationship between precursor concentration, nanostructure quality, and bioactivity. This green synthesis approach not only reduces reliance on toxic chemicals but also produces structurally sound and biologically active MoO<sub>3</sub> nanoparticles. These characteristics make them promising candidates for applications in catalysis, sensing, antimicrobial coatings, and environmental remediation, aligning with sustainability goals in nanotechnology development [34].

#### 5. Conflict of Interest:

The authors declare that there are no conflicts of interest regarding the publication of this paper. The research was conducted in the absence of any commercial or financial relationships that could be construed as a potential conflict of interest.

#### 6. Acknowledgement:

The authors express their sincere gratitude to the management and administration for providing the necessary facilities and support to carry out this research work. The authors also acknowledge the laboratory staff and technical team for their assistance in material synthesis and characterization studies. Special thanks are extended to colleagues and mentors for their valuable guidance and constructive suggestions throughout the course of this study.

#### 7. References:

1. Al-Alotaibi, A.L., Altamimi, N., Howsawi, E. et al. Synthesis and Characterization of MoO<sub>3</sub> for Photocatalytic Applications. *J Inorg Organomet Polym* 31, 2017–2029 (2021).
2. Alotaibi, Amal & Altamimi, Nafla & Elsayed, Khaled & Elhassan, Asmaa. (2021). Synthesis and Characterization of MoO<sub>3</sub> for Photocatalytic Applications. *Journal of Inorganic and Organometallic Polymers and Materials*. 31. 3904.

3. Indrakumar J, Balan P, Murali P, Solaimuthu A, Vijayan AN, Korrapati PS. Applications of molybdenum oxide nanoparticles impregnated collagen scaffolds in wound therapeutics. *J Trace Elem Med Biol.* 2022 Jul;72:126983.
4. Rees JD, Gorby YA, Sawyer SM. Synthesis and characterization of molybdenum disulfide nanoparticles in *Shewanella oneidensis* MR-1 biofilms. *Biointerphases.* 2020 Jul 24;15(4):041006.
5. Withanage SS, Charles V, Chamlagain B, Wheeler R, Mou S, Khondaker SI. Synthesis of highly dense MoO<sub>2</sub>/MoS<sub>2</sub> core-shell nanoparticles via chemical vapor deposition. *Nanotechnology.* 2021 Jan 29;32(5):055605.
6. Žigon J, Centa UG, Remškar M, Humar M. Application and characterization of a novel PVDF-HFP/PVP polymer composite with MoO<sub>3</sub> nanowires as a protective coating for wood. *Sci Rep.* 2023 Mar 1;13(1):3429.
7. Rashtbari S, Dehghan G, Amini M, Khorram S, Khataee A. A sensitive colorimetric/fluorimetric nanoprobe for detection of polyphenols using peroxidase-mimic plasma-modified MoO<sub>3</sub> nanoparticles. *Chemosphere.* 2022 May;295:133747.
8. Cervantes-Avilés P, Huang X, Keller AA. Dissolution and Aggregation of Metal Oxide Nanoparticles in Root Exudates and Soil Leachate: Implications for Nanoagrochemical Application. *Environ Sci Technol.* 2021 Oct 19;55(20):13443-13451.
9. Li XL, Li YD. Formation of MoS<sub>2</sub> inorganic fullerenes (IFs) by the reaction of MoO<sub>3</sub> nanobelts and S. *Chemistry.* 2003 Jun 16;9(12):2726-31.
10. Hammons JA, Wang W, Ilavsky J, Pantoya ML, Weeks BL, Vaughn MW. Small angle X-ray scattering analysis of the effect of cold compaction of Al/MoO<sub>3</sub> thermite composites. *Phys Chem Chem Phys.* 2008 Jan 7;10(1):193-9.
11. Choi YH. Molybdenum Oxide Nanoparticle Aggregates Grown by Chemical Vapor Transport. *Materials (Basel).* 2022 Mar 16;15(6):2182.
12. Piçarra S, Lopes E, Almeida PL, de Lencastre H, Aires-de-Sousa M. Novel coating containing molybdenum oxide nanoparticles to reduce *Staphylococcus aureus* contamination on inanimate surfaces. *PLoS One.* 2019 Mar 18;14(3):e0213151.
13. Ogungbesan SO, Zhou C, Kalulu M, Anselm OH, Ogunneye AL, Adedokun RA, Díaz Díaz D, Fu G. Synthesis, Characterization, and Cytotoxicity of Photochromic Molybdenum Oxide-Doped Tungsten Oxide Polymeric Nanohybrid Films for Biomedical Applications. *Chemphyschem.* 2025 Mar 24:e2400987.
14. Wang L, Li P, Yang J, Ma Z, Zhang L. Supercapacitive performance of C-axis preferentially oriented TiO<sub>2</sub> nanotube arrays decorated with MoO<sub>3</sub> nanoparticles. *Phys Chem Chem Phys.* 2023 Apr 5;25(14):10063-10070.
15. De A, Datta J, Haldar I, Biswas M. Catalytic Intervention of MoO<sub>3</sub> toward Ethanol Oxidation on PtPd Nanoparticles Decorated MoO<sub>3</sub>-Polypyrrole Composite Support. *ACS Appl Mater Interfaces.* 2016 Oct 26;8(42):28574-28584.
16. Asundi AS, Hoffman AS, Bothra P, Boubnov A, Vila FD, Yang N, Singh JA, Zeng L, Raiford JA, Abild-Pedersen F, Bare SR, Bent SF. Understanding Structure-Property Relationships of MoO<sub>3</sub>-Promoted Rh Catalysts for Syngas Conversion to Alcohols. *J Am Chem Soc.* 2019 Dec 18;141(50):19655-19668.
17. Bhaumik S, Pal AJ. Light-emitting diodes based on solution-processed nontoxic quantum dots: oxides as carrier-transport layers and introducing molybdenum oxide nanoparticles as a hole-inject layer. *ACS*

- Appl Mater Interfaces. 2014 Jul 23;6(14):11348-56.
18. Naeimi A, Honarmand M, Sedri A. Ultrasonic assisted fabrication of first MoO<sub>3</sub>/copper complex bio-nanocomposite based on Sesbania sesban plant for green oxidation of alcohols. Ultrason Sonochem. 2019 Jan;50:331-338.
  19. Alghamdi, Badr. (2020). MoO<sub>3</sub> Nano-Bricks as Novel Antimicrobial Agents. European Journal of Biology and Biotechnology.
  20. Lopes E, Piçarra S, Almeida PL, de Lencastre H, Aires-de-Sousa M. Bactericidal efficacy of molybdenum oxide nanoparticles against antimicrobial-resistant pathogens. J Med Microbiol. 2018 Aug;67(8):1042-1046.
  21. Piçarra S, Lopes E, Almeida PL, de Lencastre H, Aires-de-Sousa M. Novel coating containing molybdenum oxide nanoparticles to reduce Staphylococcus aureus contamination on inanimate surfaces. PLoS One. 2019 Mar 18;14(3):e0213151.
  22. Nunna, Guru Prakash, Siddarapu, Himagirish Kumar, Nimmagadda, Venkata Vijaya Jyothi, Obili, Mahammad Hussain, Ko, Tae Jo, Lim, Jiseok, Choi, Jungwook, Biogenic Synthesis of High-Performance  $\alpha$ -MoO<sub>3</sub> Nanoparticles from Tryptophan Derivatives for Antimicrobial Agents and Electrode Materials of Supercapacitors, International Journal of Energy Research, 2023, 6715319, 15 pages, 202.
  23. Fakhri A, Nejad PA. Antimicrobial, antioxidant and cytotoxic effect of Molybdenum trioxide nanoparticles and application of this for degradation of ketamine under different light illumination. J Photochem Photobiol B. 2016 Jun;159:211-7.
  24. Swamy, M.M., Giresha, A.S., Rao, S. et al. Eco-friendly development of Leucas aspera-derived MoO<sub>3</sub> nanoparticles: corrosion studies and multifunctional applications in medicine, agriculture, and industry. Appl. Phys. A 131, 71 (2025).
  25. Bharathidasan P, Surya M, Geetha Sravanthy P, Saravanan M. Green Synthesis of Molybdenum Nanoparticles From Solanum xanthocarpum and Evaluation of Their Antimicrobial and Antioxidant Activity Against Multidrug-Resistant Wound Isolates. Cureus. 2024 Mar 23;16(3):e56760.
  26. Salim, A., & Sadhasivam, S. (2023). Biofabricated MoO<sub>3</sub> nanoparticles for biomedical applications: Antibacterial efficacy, hemocompatibility, and wound healing properties. Nano and Medical Materials, 3(1).
  27. Amiri MR, Alavi M, Taran M, Kahrizi D. Antibacterial, antifungal, antiviral, and photocatalytic activities of TiO<sub>2</sub> nanoparticles, nanocomposites, and bio-nanocomposites: Recent advances and challenges. Journal of Public Health Research. 2022;11(2).
  28. Ashwini, M.A. et al. (2024). Biogenic Metal Nanoparticles for Antibacterial and Antifungal Applications and Their Challenges. In: Garg, S., Chandra, A., Sagadevan, S. (eds) Emerging Sustainable Nanomaterials for Biomedical Applications. Springer, Cham.
  29. Annu & Akbar, Ali & Ahmed, Shakeel. (2019). Green Synthesis of Metal, Metal Oxide Nanoparticles, and Their Various Applications.
  30. Kobayashi RKT, Bohara RA, Rai M, Nakazato G. Editorial: Green synthesis of metallic and metal oxide nanoparticles with biological applications. Front Chem. 2025 Jan 6;12:1546838.
  31. Khan F, Shariq M, Asif M, Siddiqui MA, Malan P, Ahmad F. Green Nanotechnology: Plant-Mediated Nanoparticle Synthesis and Application. Nanomaterials (Basel). 2022 Feb 17;12(4):673.
  32. Wang J, Jiang Z, Peng G, Hoenig E, Yan G, Wang M, Liu Y, Du X, Liu C. Surface Valence State Effect of MoO<sub>2+x</sub> on Electrochemical Nitrogen Reduction. Adv Sci (Weinh). 2022 Apr;9(12):e21048

57.

33. Ma F, Yuan A, Xu J, Hu P. Porous  $\alpha$ -MoO<sub>3</sub>/MWCNT nanocomposite synthesized via a surfactant-assisted solvothermal route as a lithium-ion-battery high-capacity anode material with excellent rate capability and cyclability. *ACS Appl Mater Interfaces*. 2015 Jul 22;7(28):15531-41.
34. Zhu Y, Yao Y, Luo Z, Pan C, Yang J, Fang Y, Deng H, Liu C, Tan Q, Liu F, Guo Y. Nanostructured MoO<sub>3</sub> for Efficient Energy and Environmental Catalysis. *Molecules*. 2019 Dec 19;25(1):18.